Dipeptidyl Peptidase 4 Inhibitors

Subjects: Pharmacology & Pharmacy

Contributor: Anna Gumieniczek , Anna Berecka-Rycerz

Information on absorption, metabolism and excretion of drugs is necessary to support the studies on their pharmacokinetics and potential drug–drug interactions. Moreover, the knowledge on drug metabolism is one of the crucial factors used to assess their pharmacokinetic profile in patients with some dysfunctions. It is especially important in diabetic patients with higher incidence of chronic liver and kidney problems.

drug metabolism and drug degradation | chromatographic and radiometric methods | dedicated packings | DPP-4

1. Introduction

Gliptins have been developed to prevent degradation of endogenously released incretins, glucose-dependent insulinotropic polypeptide (GIP) and glucagon-like peptide 1 (GLP-1), by dipeptidyl peptidase 4 (DPP-4) enzyme. Thus, they act as DPP-4 inhibitors and prolong respective actions of these endogenous incretins. They do not pass the blood–brain barrier, have no direct effect on satiety, and in contrast with GLP-1 receptor agonists (GLP-1 RAs), did not alter gastric emptying. However, when compared with GLP-1 RAs, the DPP-4 inhibitors offer several advantages such as oral administration, absence of gastrointestinal adverse effects and lower costs. What is more, some clinical data suggest that gliptins could exert positive cardiovascular effects. Because of their safety profile, especially their very low risk of hypoglycemia, gliptins could be indicated in elderly patients [1][2].

Five of these DPP-4 inhibitors, i.e., anagliptin (ANA, N-[2-[[2-[(2S)-2-cyanopyrrolidin-1-yl]-2-oxoethyl]amino]-2-methylpropyl]-2-methylpyrazolo[1,5-a]pyrimidine-6-carboxamide) (approved in Japan), alogliptin (ALO, 2-{[6-(3-aminopiperidin-1-yl)-3-methyl-2,4-dioxo-3,4-dihydropyrimidin-1(2H)-yl]methyl}benzonitrile), linagliptin (LINA, 8-[(3R)-3-aminopiperidin-1-yl]-7-but-2-ynyl-3-methyl-1-[(4-methylquinazolin-2-yl)methyl]purine-2,6-dione), sitagliptin (SITA, (3S)-3-amino-1-[3-(trifluoromethyl)-5,6-dihydro[3][4][5]triazolo[4,3-a]pyrazin-7(8H)-yl]-4-(2,4,5-trifluorophenyl)butan-1-one), saxagliptin (SAXA, (1S,3S,5S)-2-[(2S)-2-amino-2-(3-hydroxyadamantan-1-yl)acetyl]-2-azabicyclo[3.1.0]hexane-3-carbonitrile) and vildagliptin (VILDA, (2S)-1-{[(3-hydroxyadamantan-1-yl)amino]acetyl}pyrrolidine-2-carbonitrile) (FDA approved), teneligliptin (TENE, [(2S,4S)-4-[4-(5-methyl-2-phenylpyrazol-3-yl)piperazin-1-yl]pyrrolidin-2-yl]-(1,3-thiazolidin-3-yl)methanone) (approved in Japan, South Korea and India [16) were introduced by regulatory authorities between 2006 and 2013, while evogliptin (EVO, (3R)-4-[(3R)-3-amino-4-(2,4,5-trifluorophenyl)butanoyl]-3-[(2-methylpropan-2-yl)oxymethyl]piperazin-2-one) was approved in South Korea in 2015. Omarigliptin (OMA, (2R,3S,5R)-2-(2,5-difluorophenyl)-5-[2-(methanesulfonyl)-2,6-dihydropyrrolo[3,4-c]pyrazol-5(4H)-yl]oxan-3-amine) and trelagliptin (TRELA, 2-({6-[(3R)-3-aminopiperidin-1-yl]-3-

methyl-2,4-dioxo-3,4-dihydropyrimidin-1(2H)-yl}methyl)-4-fluorobenzonitrile) are the DPP-4 inhibitors approved in Japan in 2015 as the first once-weekly oral antidiabetic agents in the world [6].

Gliptins can be classified into peptidomimetic (i.e., ANA, OMA, SAXA, SITA, TENE and VILDA) and non-peptidomimetic (i.e., ALO, EVO, LINA and TRELA) subtypes. Due to their specificity to the substrate site of the enzyme, some of them have substituted pyrrolidines or thiazolidines as a proline mimetic moiety. Although their chemical structures differ from each other, all DPP-4 inhibitors are substrate-competitive active site binders and have common interactions with the key residues of the target protein [2]. Based on the half-life and time of dissociation from the DPP-4 enzyme, they are prescribed twice a day (e.g., ANA and VILDA), once a day (e.g., ALO, EVO, LINA, SITA, SAXA) or once a week (e.g., OMA, TRELA) [1]. The structures of the mentioned DPP-4 inhibitors are presented in **Figure 1**.

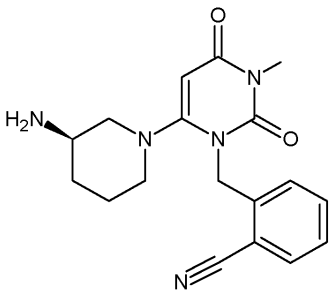

Alogliptin (ALO)

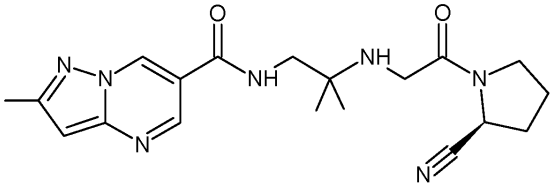

Anagliptin (ANA)

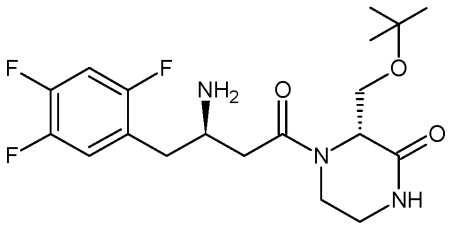

Evogliptin (EVO)

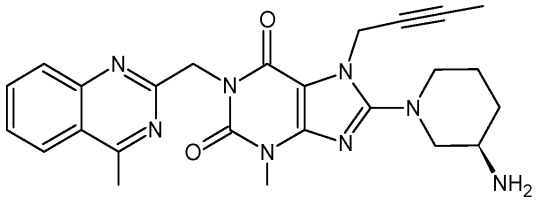

Linagliptin (LINA)

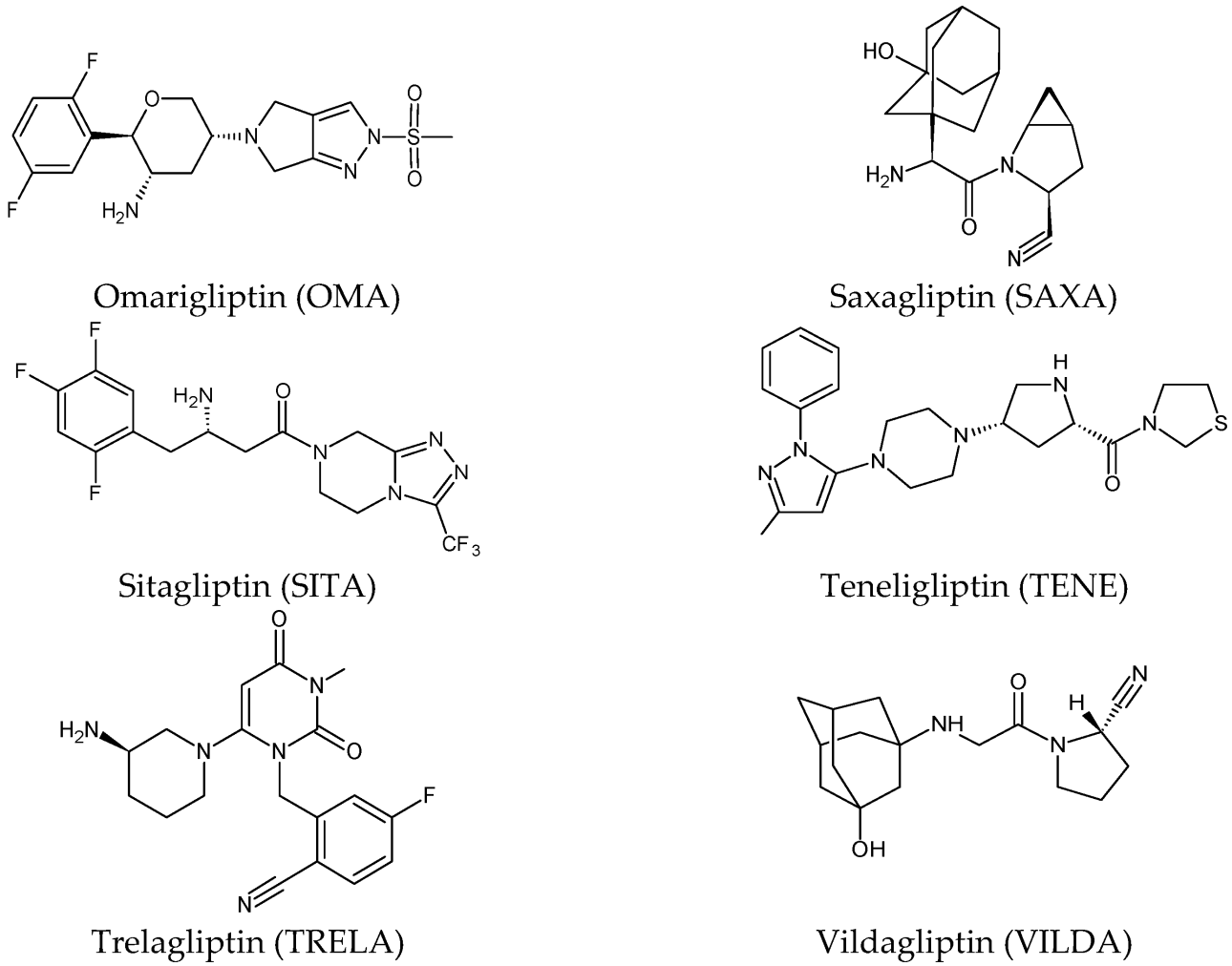

Figure 1. Chemical structures of DPP-4 inhibitors: alogliptin (ALO), anagliptin (ANA), evogliptin (EVO), linagliptin (LINA), omarigliptin (OMA), saxagliptin (SAXA), sitagliptin (SITA), teneligliptin (TENE), trelagliptin (TRELA) and vildagliptin (VILDA).

2. Metabolic Transformations of Gliptins (DPP-4 Inhibitors) and the Methods Used for Elucidating Their Metabolic Pathways

2.1. Metabolism of Gliptins

Alogliptin (ALO) is a highly potent and selective inhibitor of DPP-4 that was developed using the technology of structure-based drug design (SbDD). In the paper from the literature [7], it was shown that ca. 10% of ALO is metabolized, while 60–70% of the dose is excreted as unchanged drug in the urine. Two minor metabolites were detected following oral administration of [14C]-ALO, i.e., N-demethylated ALO (ALO-M1) (<1% of the dose) (**Table 1**) that inhibits DPP-4 similar to the parent molecule, and inactive N-acetylated ALO (<6% of the dose). It was also speculated that ALO is mainly metabolized by CYP2D6 and CYP3A4.

Because anagliptin (ANA) is not frequently used in other countries than Japan, only a small number of reports exists investigating its biological properties and pharmacokinetics. The major metabolic pathway of ANA was proposed as the cyano group hydrolysis to generate the carboxylic acid metabolite ANA-M1 (**Table 2**), which accounted for 29.2% of the dose. The parent ANA and ANA-M1 were eliminated mainly with urine where the mechanisms of the active transport were probably involved [8].

More information on the possible metabolic pathways of evogliptin (EVO) in humans was reported. Metabolism of EVO was proposed as the phase I reactions where the drug is metabolized to 4-oxo-EVO (EVO-M1), 4(S)-hydroxy-EVO (EVO-M2) and 4(R)-hydroxy-EVO (EVO-M3) (**Table 1**), and as the II phase reactions forming 4(S)-hydroxy-EVO glucuronides and EVO-N-sulfates. At the same time, formation of EVO-M2 and EVO-M3 was inhibited by the CYP3A4 antibody, suggesting that CYP3A4 played a major role in the metabolism of EVO. It was also shown that EVO-M2 could be further metabolized to respective glucuronides by UDP-glucuronosyltransferases UGT2B4 and UGT2B7 [9].

The above data on EVO were confirmed in the next study from the literature [10]. The metabolism of EVO was also shown by the phase I reactions, i.e., hydroxylation and oxidation, as well as by opening of piperazine ring and oxidation, forming EVO-M4, EVO-M5 and EVO-M6 (**Table 1**). In addition, the phase II reactions were shown to be involved, i.e., glucuronidation, sulfation, and conjugation with glycine–cysteine moieties.

The chemical structure of linagliptin (LINA) is based on xanthine moiety that distinguishes this drug from other gliptins. It may offer some differences in pharmacokinetic and pharmacodynamic properties of LINA, e.g., its low dissociation from the enzyme and greater potency than other gliptins. It is known that LINA is predominantly eliminated unchanged after both oral and intravenous administration [2]. However, the inactive metabolite LINA-M1 was identified in plasma as a major metabolite after oral administration. A two-step mechanism was proposed for its formation, i.e., CYP3A4-dependent conversion of the secondary amine of the parent drug to the corresponding ketone via oxidative deamination, followed by reduction. In excreta, the main metabolite after oral and intravenous administration was LINA-M2 formed by hydroxylation of the methyl group of the butinyl side chain. Next, minor metabolites could be formed by combinations of the following reactions: oxidation of the butinyl side chain and the piperidine moiety followed by oxidative degradation of the piperidine moiety, and finally N-acetylation and glucuronidation. The oxidation of the methyl group at position 4 of the quinazoline moiety was also proposed, and resulted in the corresponding carboxylic acid metabolite LINA-M3 (**Table 1**). A cysteine adduct and its sulfate conjugate were additionally observed in urine after intravenous administration of LINA [11].

In the study of Xu et al. [12], absorption, metabolism and excretion of omarigliptin (OMA) were evaluated in healthy male subjects after a single oral dose of 25 mg of [14C]-OMA. Radioactivity levels in plasma and excreta were determined via accelerator mass spectrometry (AMS). As a result, minimal metabolism of OMA was observed, as indicated by the fact that the parent drug accounted for ca. 89% of the radioactivity in urine. However, some oxidative metabolites were detected in plasma, with each comprising less than 3% of the total radioactivity.

Table 1. Metabolites of DPP-4 inhibitors produced by the phase I reactions: alogliptin (ALO), anagliptin (ANA), evogliptin (EVO), linagliptin (LINA), saxagliptin (SAXA), sitagliptin (SITA), teneligliptin (TENE) and vildagliptin

(VILDA).

Metabolite	Structure	*m/z* $[M + H]^+$	Ref.
ALO-M1	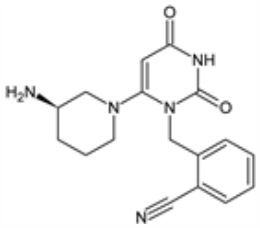	n.a.	[7]
ANA-M1	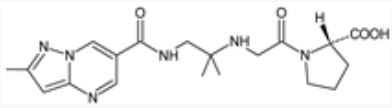	366 *	[8]
EVO-M1	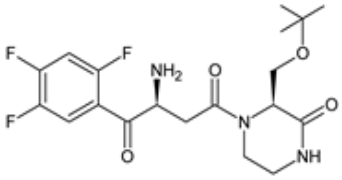	416 *	[9]
EVO-M2 EVO-M3 (isomers)	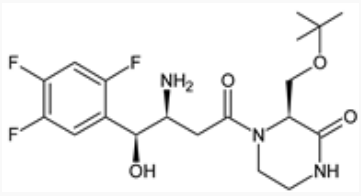	418 *	[9][10]
EVO-M4	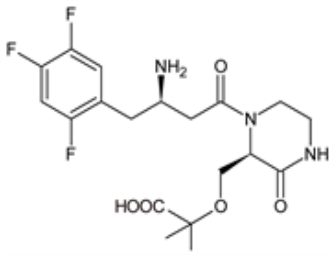	418 *	[10]
EVO-M5	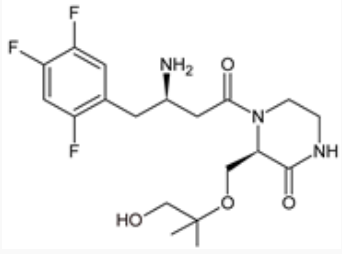	432 *	[10]

A few metabolites of sitagliptin (SITA) were detected, e.g., diketone metabolite SITA-M1. In addition, hydroxylation of both amine group and aromatic ring followed by formation of glucuronide metabolites, as well as oxidation of NH2 and hydroxylation followed by loss of HF to form SITA-M2, was proposed (**Table 1**). On the other hand, it was clearly shown that only 3.1% of the parent drug was metabolized over 2 h incubation [17].

Metabolite	Structure[17]	*m/z* $[M + H]^+$	Ref.
EVO-M6	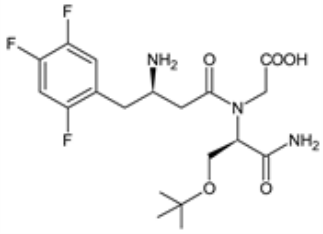	434 *	[10]
LINA-M1	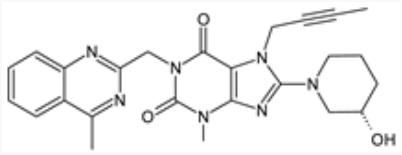	n.a.	[2]
LINA-M2	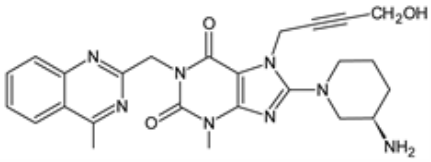	n.a.	[11]
LINA-M3	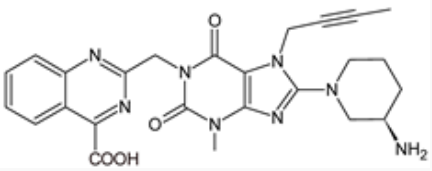	n.a.	[11]
SAXA-M1	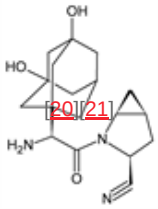	332 *	[13][14][15]
SITA-M1	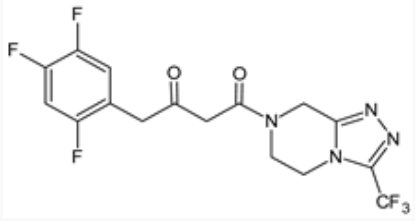	408 *	[16]
SITA-M2	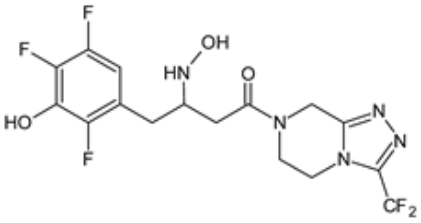	422 *	[16]

[18]

[2]

[20][21]

-SITA and
MS, using
oducts of
proposed
rved that

excreted
ENE were
enase 3
TENE-M2
TENE-M4
lroxylated

near 70%
able 1) is
bolites of
the major

LO, LINA,
to initiate
shown for
y, rapidly
the nitrile
ANA have
redictable

etric and
ase were
omparing

the LC retention times and MS spectra with respective synthetic standards allowed identification of some of the detected metabolites [8].

To identify EVO and its metabolites in human liver microsomes, an orbitrap mass spectrometer coupled with the UPLC system was used. Separation was performed on a C8 column using gradient elution. A higher-energy

Metabolite	Structure	*m/z* $[M + H]^+$	Ref.
SITA-M3	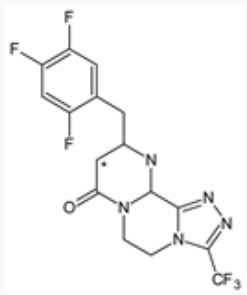	406 *	[17]
TENE-M1	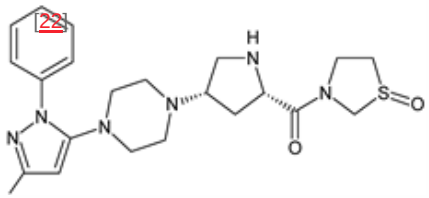	443 *	[18][19]
TENE-M2	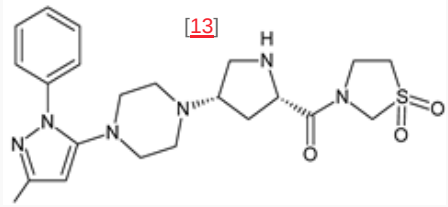	n.a.	[18]
TENE-M3	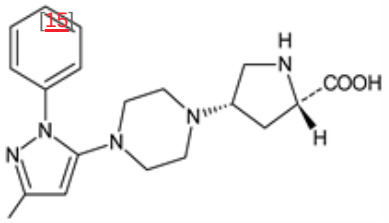	n.a.	[18]
TENE-M4	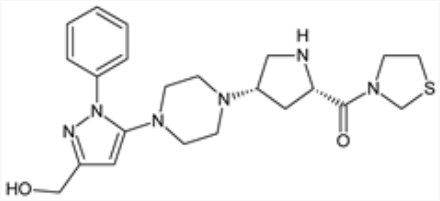	n.a.	[18]
TENE-M5	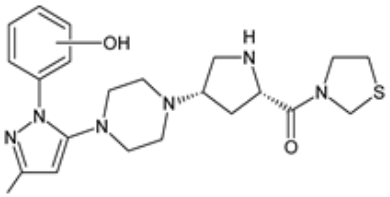	n.a.	[18]
VILDA-M1	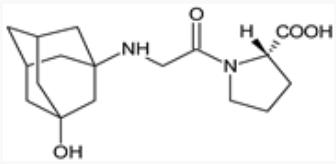	n.a.	[2]

[12] [9] [10] [22] [13] [14] [15] [16] [18] [23]

Next, a rapid and sensitive LC–MS/MS method for the quantification of TENE and its active metabolite, TENE-M1, in human plasma was elaborated by Park et al. [19], using deuterated TENE as an internal standard. This method was proposed as an alternative to the AMS method described above [18], in order to avoid its disadvantages, including its complicated procedure and the expense of designing the radioactive isotope (**Table 2**).

Table 2. LC and LC-MS methods for determination of metabolites of gliptins: anagliptin (ANA), evogliptin (EVO), linagliptin (LINA), omarigliptin (OMA), saxagliptin (SAXA), sitagliptin (SITA), teneliglitin (TENE) and vildagliptin (VILDA).

Compound	Conditions	Ref.
ANA	C18 column (2.0 × 150 mm, 3 µm) and isocratic elution using 1% CH_3COOH/ACN (80:20, *v*/*v*), 1.0 mL/min; MS/MS with positive ESI. C18 column (4.6 × 250 mm, 5 µm) and gradient elution: (A) 50 mM ammonium acetate, (B) ACN, 1.0 mL/min.	[8]
EVO	Unison-C8 column (2.0 × 75 mm, 3.0 µm) and gradient elution of A) 5% ACN in 0.1% HCOOH and B) 95% ACN in 0.1% HCOOH, 0.3 mL/min. The column and autosampler temperatures: 40 °C and 6 °C; ESI in positive and negative mode: spray voltage, 4.0 kV in positive mode and −3.0 kV in negative mode; vaporizer temperature, 350 °C; capillary temperature, 330 °C; sheath gas pressure, 35 Arb; and auxiliary gas pressure, 15 Arb; collision energy of 10 to 40 eV.	[9]
EVO	Kinetex C18 column (4.6 × 150 mm, 2.6 µm) and gradient elution with (A) 20 mM ammonium acetate (pH 4) and (B) ACN, 1 mL/min. The column temperature 40 °C and UV detection at 268 nm. ESI in the positive mode: spray voltage, 4.5 kV; vaporizer temperature, 350 °C; capillary temperature, 330 °C; sheath gas pressure, 50 Arb; auxiliary gas pressure, 10 Arb; and sweep gas pressure, 5 Arb, the collision gas He, and the normalized collision energy during product ion scanning 35%.	[10]
OMA	ACE 5 C8 column (4.6 × 250 mm; 5 µm) and gradient elution with (A) 2 mM ammonium acetate in ACN:H_2O (5:95) containing 0.1% HCOOH, and (B) 2 mM ammonium acetate in ACN:H_2O (95:5) containing 0.1% HCOOH, 1.0 mL/min; N_2 as the nebulizer and auxiliary gas, and Ar as the collision gas. The ESI capillary voltage 1.2 kV. The source and desolvation temperatures 100 and 550 °C; collision energy from 20 to 30 eV.	[12]
SAXA	ACE CN column (4.6 × 150 mm, 5 µm) and ACN and 10.0 mM ammonium formate buffer of pH 5.0 (80:20, *v*/*v*); triple quadrupole MS detection with positive ESI.	[13]
SAXA	C18 column (2.1 × 50 mm, 5 µm) and gradient elution with (A) 0.1% HCOOH in H_2O and (B) 0.1% HCOOH in ACN. TurboIonSpray® source, positive ionization mode, using SRM. N_2 as the nebulizer, curtain and collision gas; 450 °C for TIS interface, 5000 V setting for ion spray voltage, 30 setting for the curtain gas and nebulizer gas.	[14]
SAXA	HILIC Chrom Matrix HP amide column (3.0 × 100 mm, 5 µm), ACN and 5 mM ammonium formate buffer containing 0.1% HCOOH. Ion spray voltage 5500 V, ion spray temperature	[15]

Compound	Conditions	Ref.
	550 °C, ion source gas 1: 50 Arb, ion source gas 2: 55 Arb, curtain gas (N_2) 30 Arb, collision gas (N_2) 10 Arb, entrance potential 10 V, collision cell exit potential 12 V.	
SITA	ZIC-HILIC column (4.6 mm × 150 mm, 5 µm) and gradient elution with (A) HCOOH in H_2O (0.1% *v*/*v*) and (B) HCOOH (0.1% *v*/*v*) in ACN, 0.3 mL/min. The capillary temperature 250 °C, spray voltage +4.5 kV and the sheath and auxiliary gas (N_2) flow rates 45 and 15. CID voltage of 40 eV.	[16]
TENE	CAPCELL PAK C18 UG120 column (4.6 × 250 mm, 5 µm,) at 40 °C and gradient elution with (A) 20 mM ammonium acetate and (B) ACN, 0.8 mL/min; positive ESI at 3800 V and CID at the collision energy of 35%.	[18]
TENE	CAPCELL Pak C18 column (2.0 × 2150 mm, 5 µm) and isocratic elution with ACN, MeOH and H_2O, 025 mL/min; temperature of the column and autosampler 50 °C and 10 °C. MS: collision gas 5 psi, curtain gas 10 psi, ion source gas (nebulizer) 30 psi, ion spray voltage 5500 V, and collision energy of 37 eV for TENE; declustering potential, entrance potential, and collision exit potential were 106 V; ESI positive ion mode using MRM.	[19]
ANA ALO LINA SITA VILDA	UPLC system and a QQQ mass spectrometer equipped with a switching valve; XBridge C18 column (2.1 × 50 mm, 3.5 µm) and gradient with (A) 0.5 mM ammonium hydrogen carbonate and (B) MeOH for VILDA or (A) 1 mM ammonium acetate and (B) ACN (B) for ANA, ALO, SITA and LINA; 0.55 mL/min. The autosampler 4 °C. ESI positive ion mode using MRM transitions. Orbitrap Fusion MS system coupled with a HPLC system: XBridge C18 column (4.6 × 100 mm, 5 µm) and gradient elution with (A) 20 mM ammonium acetate (A) and (B) ACN (B), 1.0 mL/min; ESI positive and negative ion mode.	[20] [21]

yl
nsive

2. Chen, X.-W.; He, Z.-X.; Zhou, Z.-W.; Yang, T.; Zhang, X.; Yang, Y.-X.; Duan, W.; Zhou, S.-F. Clinical pharmacology of dipeptidyl peptidase 4 inhibitors indicated for the treatment of type 2 diabetes mellitus. Clin. Exp. Pharmacol. Physiol. 2015, 42, 999–1024.
3. Yao, M.; Chen, B.; Zhao, W.; Mehl, J.T.; Li, L.; Zhu, M. LC-MS differential analysis for fast and sensitive determination of biotransformation of therapeutic proteins. Drug Metab. Dispos. 2018, 46, 451–457.
4. Rakusanova, S.; Cajka, T. Current analytical methods to monitor type 2 diabetes medication in biological samples. TrAC Trends Anal. Chem. 2023, 158, 116831.
5. ICH Topic Q 3 A (R2) “Impurities in New Drug Substances”. Available online: https://www.ema.europa.eu/en/documents/scientific-guideline/ich-q-3-r2-impurities-new-drug-substances-step-5_en.pdf (accessed on 10 May 2023).
6. Ahrén, B. DPP-4 Inhibition and the Path to Clinical Proof. Front. Endocrinol. 2019, 10, 376.
7. Kaku, K.; Kisanuki, K.; Shibata, M.; Oohira, T. Benefit-risk assessment of alogliptin for the treatment of type 2 diabetes mellitus. Drug Saf. 2019, 42, 1311–1327.
8. Furuta, S.; Smart, C.; Hackett, A.; Benning, R.; Warrington, S. Pharmacokinetics and metabolism of anagliptin, a novel dipeptidyl peptidase-4 inhibitor, in humans. Xenobiotica 2013, 43, 432–442.

9. Jeong, H.U.; Kim, J.H.; Lee, D.Y.; Shim, H.J.; Lee, H.S.; McPhee, D.J. In vitro metabolic pathways of the new anti-diabetic drug evogliptin in human liver preparations. Molecules 2015, 20, 21802–21815.
10. Lee, D.Y.; Kim, J.H.; Shim, H.J.; Jeong, H.U.; Lee, H.S. Absorption, metabolism, and excretion of evogliptin tartrate in male rats and dogs. J. Toxicol. Environ. Health—A: Curr. Issues 2018, 81, 453–464.
11. ICH Topic Q 3 A (R2) “Impurities in New Drug Substances Blech, S.; Ludwig-Schwellinger, E.; Gräfe-Mody, E.U.; Withopf, B.; Wagner, K. The metabolism and disposition of the oral dipeptidyl peptidase-4 inhibitor, linagliptin, in humans. Drug Metab. Dispos. 2010, 38, 667–678.
12. Xu, S.; Tatosian, D.; Mcintosh, I.; Caceres, M.; Matthews, C.; Samuel, K.; Selverian, D.; Kumar, S.; Kauh, E. Absorption, metabolism and excretion of omarigliptin, a once-weekly DPP-4 inhibitor, in humans. Xenobiotica 2018, 48, 584–591.
13. Shah, P.A.; Shah, J.V.; Sanyal, M.; Shrivastav, P.S. LC-MS/MS analysis of metformin, saxagliptin and 5-hydroxy saxagliptin in human plasma and its pharmacokinetic study with a fixed-dose formulation in healthy Indian subjects. Biomed. Chromatogr. 2017, 31, e3809.
14. Xu, X.S.; Demers, R.; Gu, H.; Christopher, L.J.; Su, H.; Cojocaru, L.; Boulton, D.W.; Kirby, M.; Stouffer, B.; Humphreys, W.G.; et al. Liquid chromatography and tandem mass spectrometry method for the quantitative determination of saxagliptin and its major pharmacologically active 5-monohydroxy metabolite in human plasma: Method validation and overcoming specific and non-specific binding at low concentrations. J. Chromatogr. B 2012, 889–890, 77–86.
15. Peng, Y.; Chang, Q.; Yang, N.; Gu, S.; Zhou, Y.; Yin, L.; Aa, J.; Wang, G.; Sun, J. Quantitative determination of metformin, saxagliptin and 5-hydroxy saxagliptin simultaneously by hydrophilic interaction liquid chromatography-electrospray ionization mass spectrometry and its application to a bioequivalence study with a single-pill combination in human. J. Chromatogr. B Analyt. Technol. Biomed. Life Sci. 2018, 1081–1082, 109–117.
16. Khreit, O.I.G.; Grant, H.M.; Henderson, C.; Watson, D.G.; Sutcliffec, O.B. Identification of Novel Metabolic Pathways of Sitagliptin (STG) by LC/MS and LC/MS2 after incubations with rat Hepatocytes. J. Drug Metab. Toxicol. 2016, 7, 220.
17. Vincent, S.H.; Reed, J.R.; Bergman, A.J.; Elmore, C.S.; Zhu, B.; Xu, S.; Ebel, D.; Larson, P.; Zeng, W.; Chen, L.; et al. Metabolism and excretion of the dipeptidyl peptidase 4 inhibitor sitagliptin in humans. Drug Metab. Dispos. 2007, 35, 533–538.
18. Nakamaru, Y.; Hayashi, Y.; Ikegawa, R.; Kinoshita, S.; Madera, B.P.; Gunput, D.; Kawaguchi, A.; Davies, M.; Mair, S.; Yamazaki, H.; et al. Metabolism and disposition of the dipeptidyl peptidase IV inhibitor teneligliptin in humans. Xenobiotica 2014, 44, 242–253.

19. Park, J.-W.; Kim, K.-A.; Park, J.-Y. Development of a liquid chromatography/tandem-mass spectrometry assay for the simultaneous determination of teneligliptin and its active metabolite teneligliptin sulfoxide in human plasma. Biomed. Chromatogr. 2020, 34, e4721.
20. Mizuno, K.; Takeuchi, K.; Umehara, K.; Nakajima, M. Identification of a novel metabolite of vildagliptin in humans: Cysteine targets the nitrile moiety to form a thiazoline ring. Biochem. Pharmacol. 2018, 156, 312–321.
21. Keck, B.D.; Ognibene, T.; Vogel, J.S. Analytical validation of accelerator mass spectrometry for pharmaceutical development. Bioanalysis 2010, 2, 469–485.
22. Mizuno, K.; Takeuchi, K.; Umehara, K.; Nakajima, M. Identification of novel metabolites of vildagliptin in rats: Thiazoline-containing thiol adducts formed via cysteine or glutathione conjugation. Drug Metab. Dispos. 2019, 47, 809–817.
23. Makarov, A.; Denisov, E.; Kholomeev, A.; Balschun, W.; Lange, O.; Strupat, K.; Horning, S. Performance evaluation of a hybrid linear ion trap/orbitrap mass spectrometer. Anal. Chem. 2006, 78, 2113–2120.